

Supplemental Information

Heterogeneous bone-marrow stromal progenitors drive myelofibrosis via a druggable alarmin axis

Nils B. Leimkühler, Hélène F.E. Gleitz, Li Ronghui, Inge A.M. Snoeren, Stijn N.R. Fuchs, James S. Nagai, Bella Banjanin, King H. Lam, Thomas Vogl, Christoph Kuppe, Ursula S.A. Stalmann, Guntram Büsche, Hans Kreipe, Ines Gütgemann, Philippe Krebs, Yara Banz, Peter Boor, Evelyn Wing-Yin Tai, Tim H. Brümmendorf, Steffen Koschmieder, Martina Crysandt, Eric Bindels, Rafael Kramann, Ivan G. Costa, and Rebekka K. Schneider

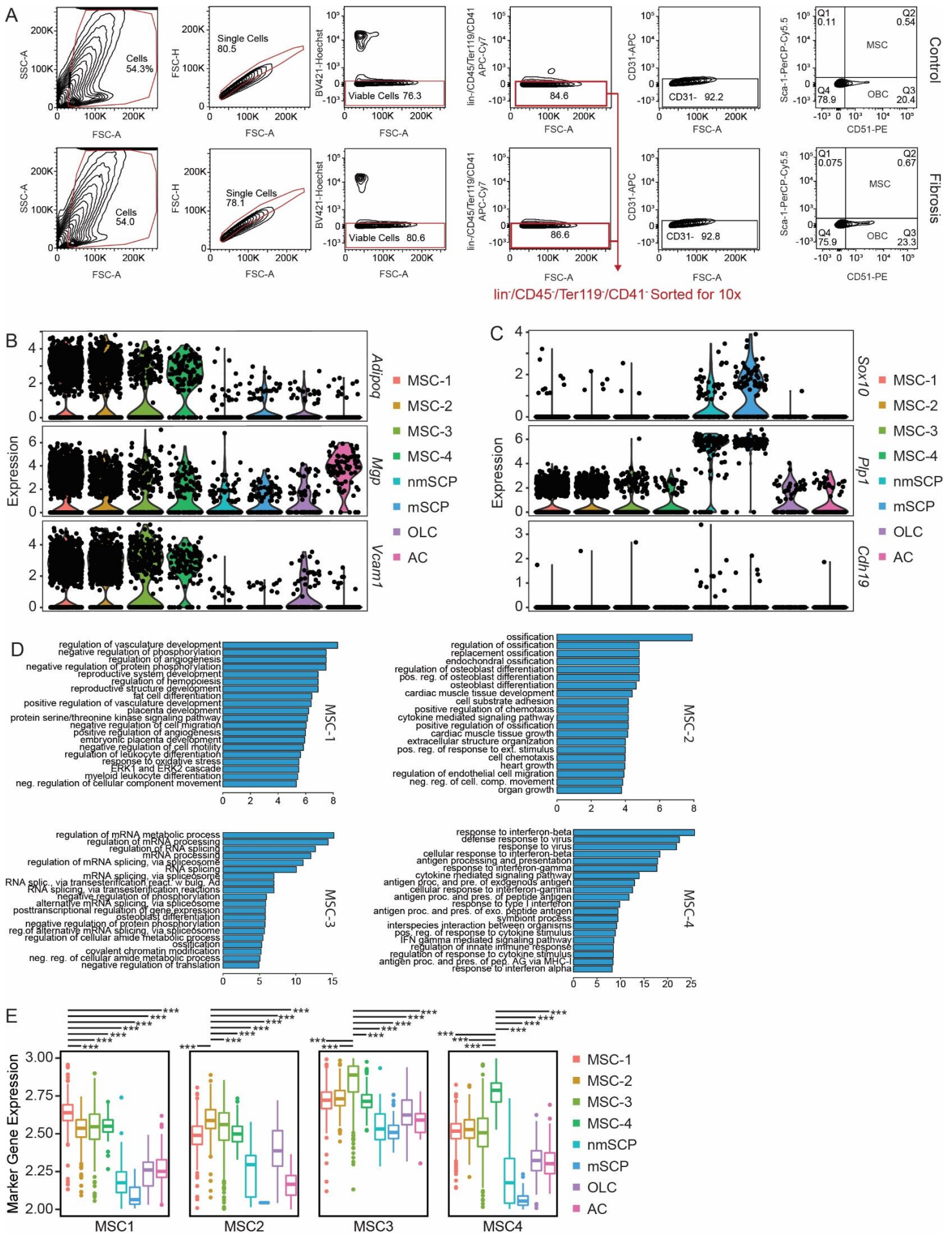


Figure S1: Sorting of non-hematopoietic cells and annotation of identified populations (related to Figure 1 and Table S2)

(A) Sorting strategy for non-hematopoietic cells. After exclusion of multiplets and dead cells, lin-CD45-Ter119-CD41- cells were sorted for scRNAseq. Staining for known niche markers (CD31-APC, CD51-PE, Sca-1-PerCP) were used as quality control. **(B)** Top GO terms corresponding to marker genes identified for the four different MSC-subclusters. GO enrichment analysis was based on clusterProfiler (Version 3.12.0). Significance is given as $-\log(p)$. **(C) (D)** Violin-plots showing the gene expression of respective marker genes per cluster of **(C)** MSCs and **(D)** SCPs. **(E)** Boxplot depicting the aggregated gene expression of respective MSC cluster marker genes in each cell population. Significance was calculated by One-Way-Anova and post-hoc pairwise t-test. The interrogated marker geneset was considered as the respective control for comparisons. p-values were adjusted according to the Benjamini-Hochberg procedure.

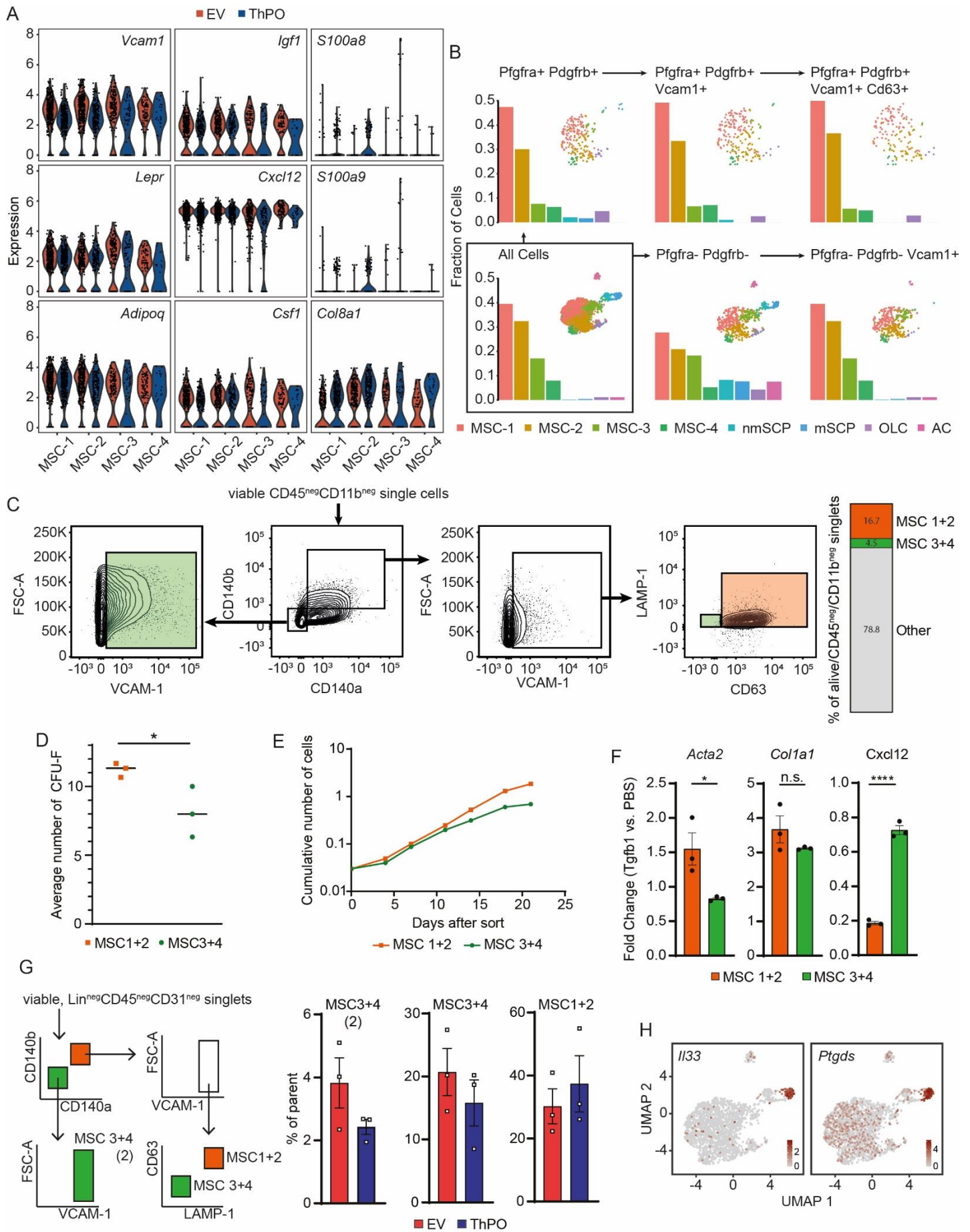


Figure S2: Changes in gene expression between ThPO/EV and functional characterization of MSC-1 and MSC-2 (related to Figure 2 and Table S3, S6)

(A) Violin-plots depicting the expression of respective differentially expressed genes as shown in Figure 2C. Expression levels in non-fibrotic (EV, red) and fibrotic conditions (ThPO, blue) are shown side by side. **(B)** Iterative

subsetting of the entire ThPO dataset on cells expressing relevant surface marker genes as previously described and found to be discriminating in the data shown. The barplot depicts the frequency of each cluster population in the respective subset. The corresponding UMAP of the subsets is depicted in the top right corner of each panel. **(C)** Sorting strategy of primary murine stromal cells. Cells were isolated from the bone chips of two wildtype mice by attachment selection. MSC-1/2 (orange) and MSC-3/4 (green) were sorted as shown. Composition of viable CD45⁻/CD11b⁻ cells is shown as stacked barplot on the right. **(D)** MSC-1/2 and MSC-3/4 were sorted as shown in (C) and immediately plated out in triplicate for the MesenCult colony assay. Colonies were counted by three independent investigators. The average count across all investigators is depicted for each replicate, black lines correspond to the mean across replicates. Significance was calculated by unpaired t-test ($p = 0.0474$). **(E)** Growth curve of sorted MSC-1/2 (orange) and MSC-3/4 (green) populations over time. **(F)** MSC-1/2 and MSC-3/4 were stimulated in triplicate with recombinant Tgf-b1 or PBS as control for 72 hours. qt-PCR was performed for *Acta2* (α -SMA), *Col1a1* and *Cxcl12*. $2^{-\Delta\Delta ct}$ -values were normalized to the respective PBS control. Values are shown as mean \pm SEM. Significance was calculated by unpaired t-test. **(G)** Bone marrow of non-fibrotic (EV, red) and fibrotic mice (ThPO, blue) was harvested at week 7.5 post transplantation. MSC-1/2 and MSC-3/4 were isolated from lineage depleted bone marrow as shown in the left panel. Values are shown as mean \pm SEM. Significance was calculated by unpaired t-test. **(H)** Expression of Interleukin-33 (*Ii33*) and Prostaglandin-H2 D-isomerase (*Ptgds*) projected onto the UMAP space of isolated cells.

on the right. **(B-C)** Volcano plot of differentially expressed genes (Wilcoxon rank sum test, two tailed; calculated per cluster individually) between TPO and EV for MSC-3, MSC-4 and non-MSC clusters. Data are shown for **(B)** Pre-Fibrosis (TPO, 4 weeks) and **(C)** Fibrosis (TPO, 8 weeks).

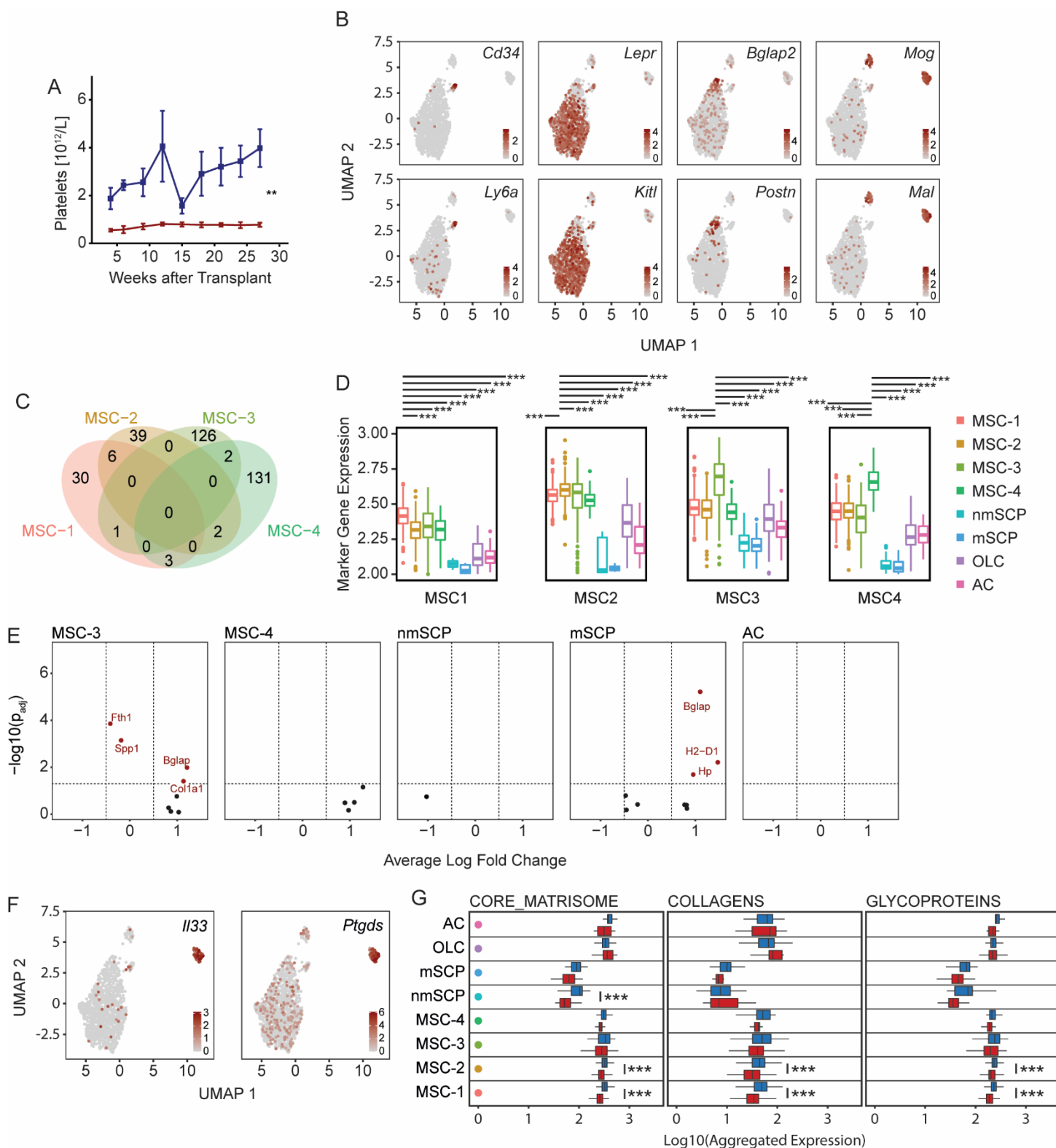


Figure S4: scRNAseq of fibrotic JAK2^{V617F} versus non-fibrotic control mice (related to Figure 4 and Table S2, S3) **(A)** Platelet counts over time after transplantation of HSPCs (mean \pm SEM). Significance was determined by Two-Way-Anova with post-hoc pairwise t-test. **(B)** Distribution of selected marker genes in the dataset as shown in Figure 4D is shown in the form of a feature plot as projection of the expression onto UMAP space. **(C)** Venn diagram depicting the count of identified top marker genes of the four identified MSC-populations. Shared markers are highlighted in intersections. **(D)** Boxplot depicting the aggregated gene expression of respective MSC cluster marker genes in each cell population. Significance was calculated by One-Way-Anova and post-hoc pairwise t-test. The interrogated marker geneset was

considered as the respective control for comparisons. p-values were adjusted according to the Benjamini-Hochberg procedure. **(E)** Volcano plot of differentially expressed genes (Wilcoxon Rank Sum Test, two-sided; calculated for each cluster individually) between JAK2^{V617F} and JAK2^{WT} for indicated cell populations. Significantly differentially expressed genes are highlighted in red. **(F)** Boxplot comparing the expression of NABA matrixome associated gene sets in each cluster and comparing the experimental (JAK2^{V617F}; blue) and control (JAK2^{WT}; red) condition. For aggregated gene expression the cumulative gene expression of each geneset per cell was normalized as described. Significance was determined by competitive gene set enrichment analysis. **(G)** Feature plot of *Irf3* and *Ptgds*. Computed expression is projected onto the UMAP space.

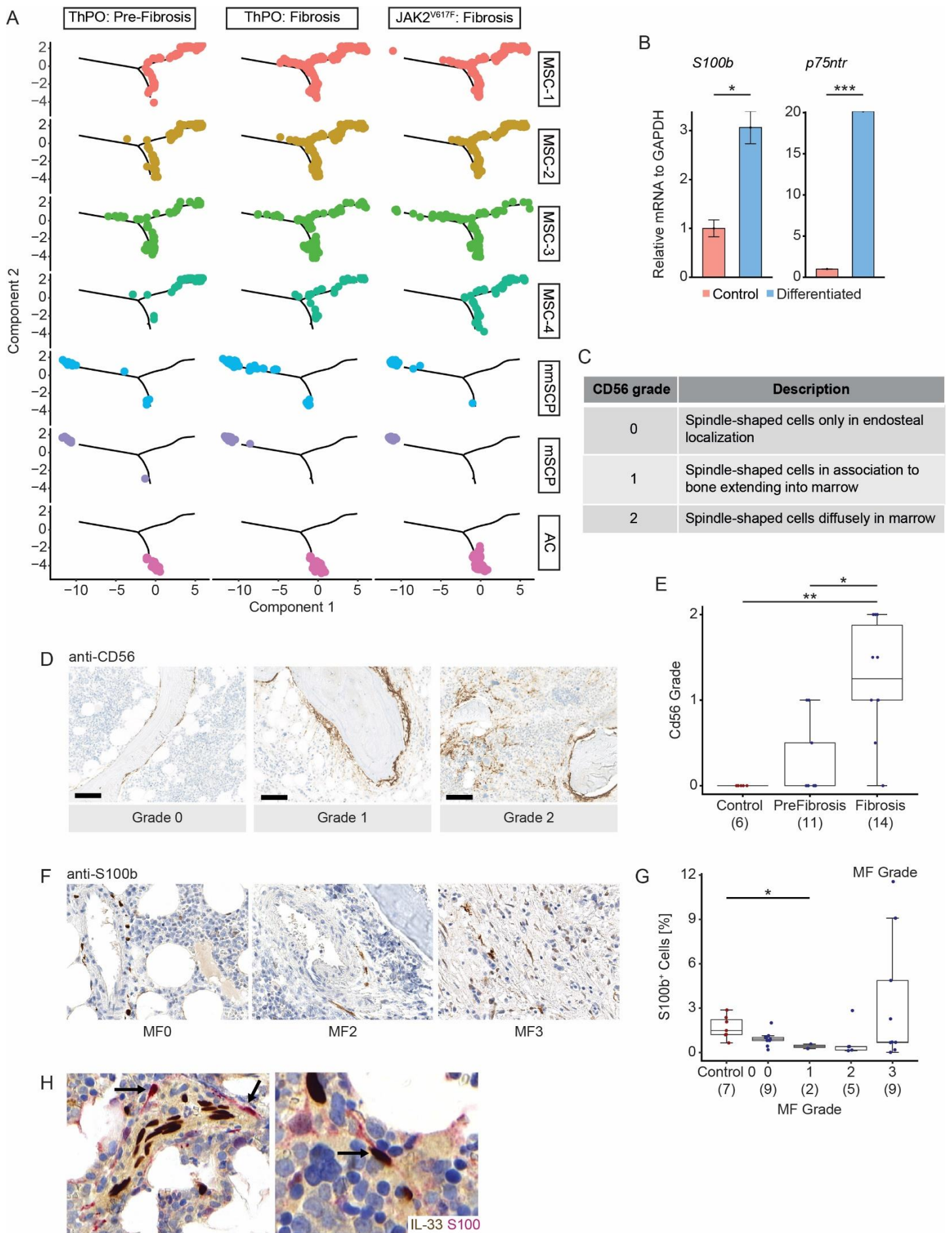


Figure S5: Ligand-Receptor and Pseudotime Analysis of non-hematopoietic clusters in different models of myelofibrosis (related to Figure 5 and Table S6)

(A) Reconstructed cell differentiation trajectory of MSC populations, coloured by cluster identity. Trajectory is shown for every experimental condition (ThPO: Pre-Fibrosis, ThPO:Fibrosis, JAK2V617F: Fibrosis) and each non-hematopoietic cluster individually. **(B)** murine MSCs were isolated and cultured as described before induction of differentiation into Schwann Cell-like cells. Relative mRNA Expression to GAPDH levels was calculated following the $2^{\Delta\Delta CT}$ -method. Significance was estimated by unpaired t-test. **(C)** Semiquantitative grading of CD56 staining in human bone marrow slides as established on the available cohort. **(D)** Representative images of respective CD56-grades as described in C. Scale bar is set at 100 μ m. **(E)** Comparison of the CD56 grade across different stages of MF. Grading was assessed by two independent researchers. Depicted is the mean of both assessments for each available patient. Significance was estimated by Kruskal-Wallis H test with *post-hoc* Wilcoxon rank sum test. p-values were adjusted for multiple hypothesis testing by the Holm-Bonferroni method. **(F)** Representative images of S100b staining in human bone marrow with varying degrees of bone marrow fibrosis. **(G)** Comparison of the relative frequency of S100+ spindle shaped cells in the bone marrow across different MF grades as shown in (F). Significance was estimated by Welch's ANOVA with *post-hoc* Games-Howell test. **(H)** Immunohistochemical co-staining of IL-33 and S100b showing S100+IL33+ cells (black arrows) in spatial association to arterioles and interspaced between hematopoietic tissue.

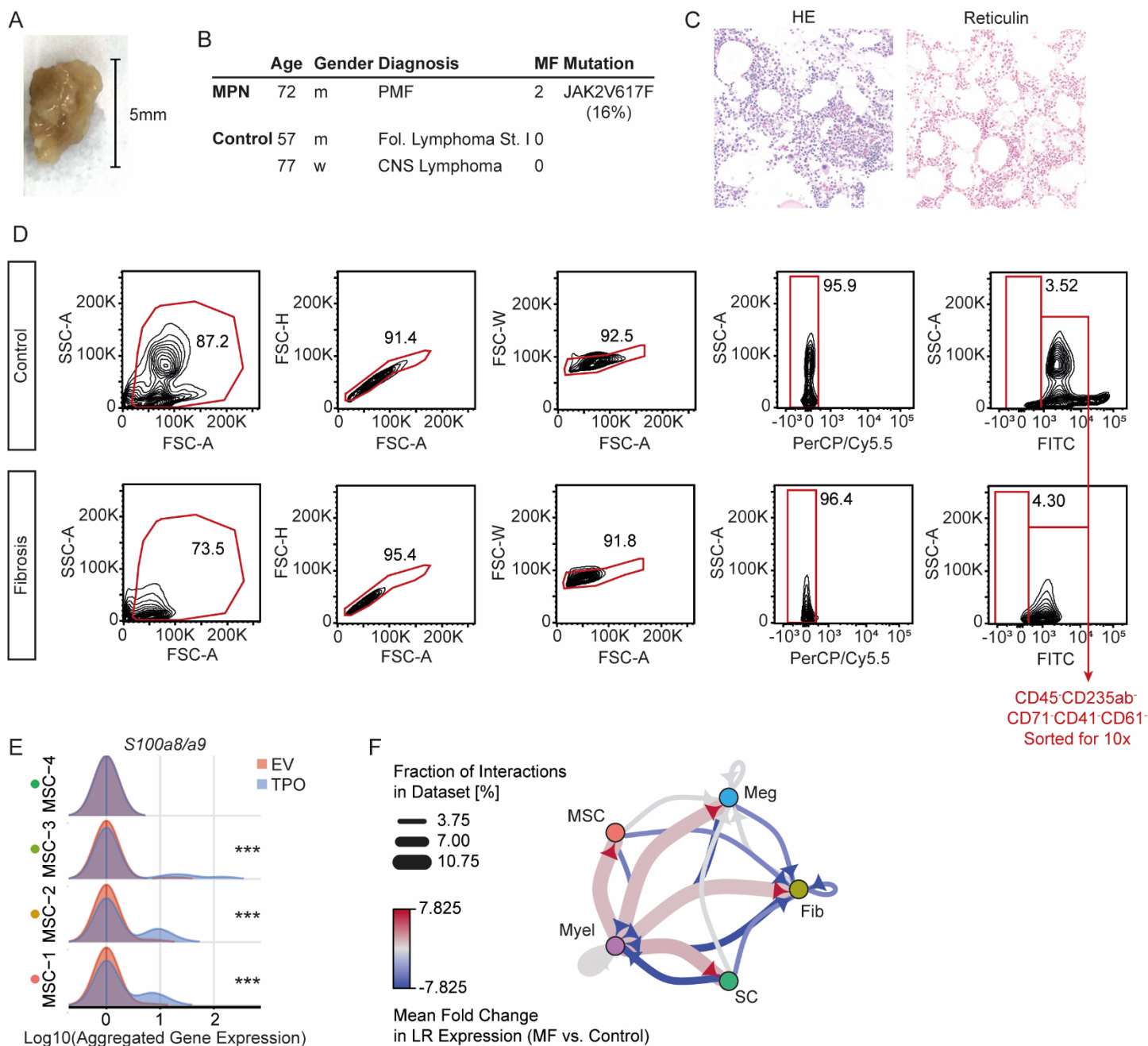


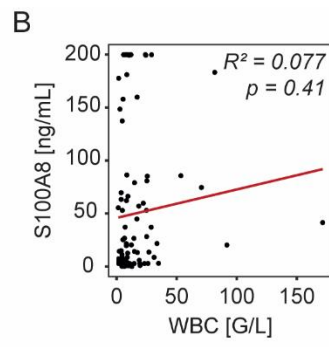
Figure S6: scRNA-sequencing of human fibrotic and non-fibrotic bone marrow shows similar changes in transcription (related to Figure 6 and Table S5)

(A) Representative image of a native bone marrow biopsy used for isolation of non-hematopoietic cells which were subsequently subjected to scRNAseq. **(B)** Clinical information about the patients whose bone marrow was used for single cell transcriptomics. **(C)** Diagnostic HE and reticulin staining of control patient 2. **(D)** Sorting strategy for non-hematopoietic cells. After exclusion of multipllets and non-viable cells, CD45⁻CD235ab⁻CD71⁻CD41⁻CD61⁻ cells were sorted for

scRNAseq. **(E)** Ridgeline plot depicting the expression of *S100a8/a9* in ThPO induced MF (blue) or murine control bone marrow (EV, red). Significance was estimated by modelling the dropout rate as a binomial process with the observed dropout rate per condition as estimator of p for both conditions respectively. **(F)** Network plot showing the mean fold change in S100A8/S100A9 ligand-receptor activity between clusters comparing those derived from fibrotic patient bone marrow to non-fibrotic control bone marrow. Interactions were estimated via CellPhoneDB. Changes in ligand-receptor activity were calculated as the mean of the fold change in ligand expression and in receptor expression comparing fibrotic and control condition. The weight of the edges depicts the number of interactions between two connected nodes divided by the overall number of inferred interactions in the dataset.

A

	MPN	CTRL
n	139	86
age (years)	60.41 (± 1.05)	53.68 (± 3.13)
gender (f/m)	54(38%)/62(44%)	26(29%)/24(27%)
<hr/>		
PMF	69(49%)	
ET	33(23%)	
PV	30(21%)	
MPN-U	7(5%)	
<hr/>		
JAK2V617F	88(63%)	
CALRdel52	24(17%)	
CALRins5	7(5%)	
MPLW515L	6(4%)	
JAK2 Exon 12	1(0,7%)	
Triple Negative	9(6%)	
VAF	50.53% (± 4.69%)	



C

	MPN	CTRL
n	54	9
age (years)	59.10 (± 2.40)	69.11 (± 2.76)
gender (f/m)	22(40%)/17(30%)	4(44%)/5(55%)
<hr/>		
PMF	34(62%)	
ET	7(12%)	
PV	5(9%)	
Other	9(17%)	
<hr/>		
JAK2V617F	34(62%)	
CALRindel	11(20%)	
Triple Negative	3(5%)	
VAF	43.81% (± 8.43%)	

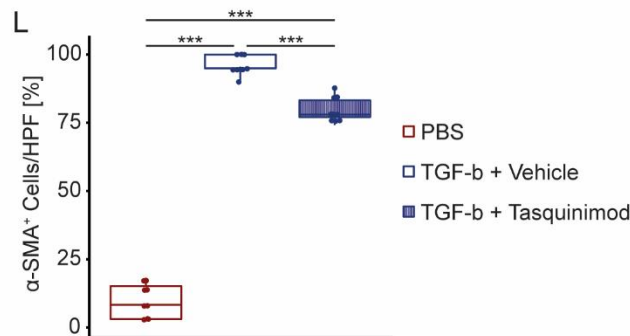
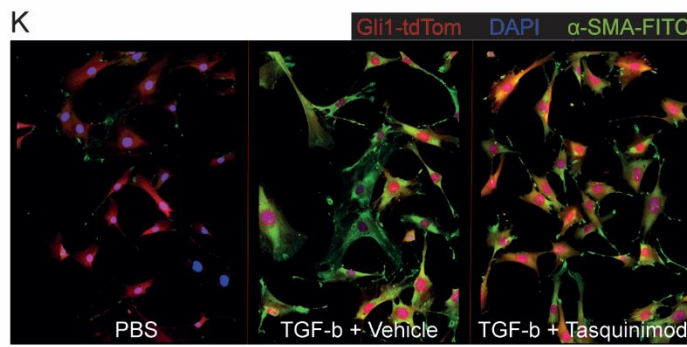
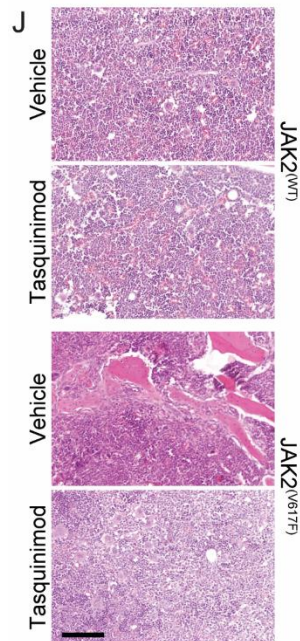
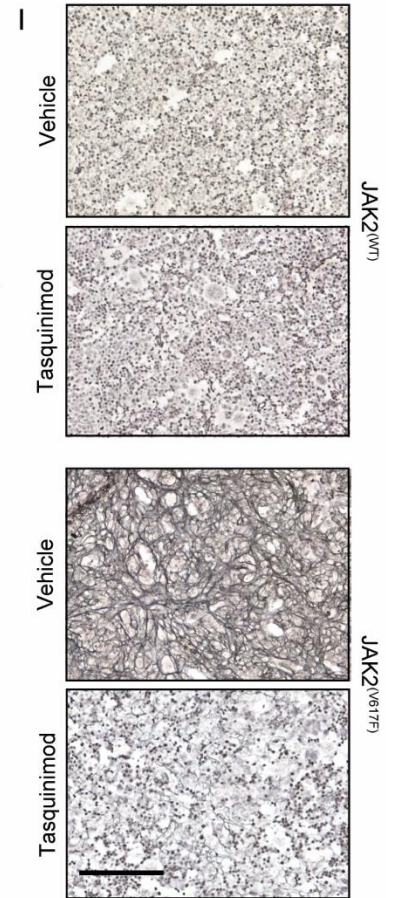
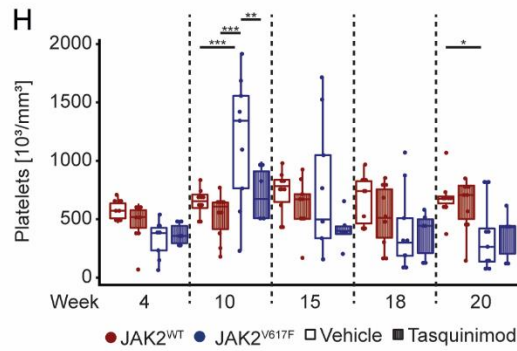
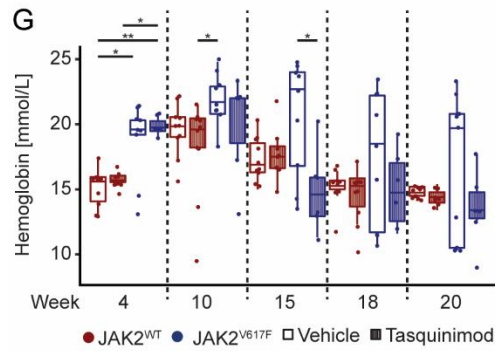
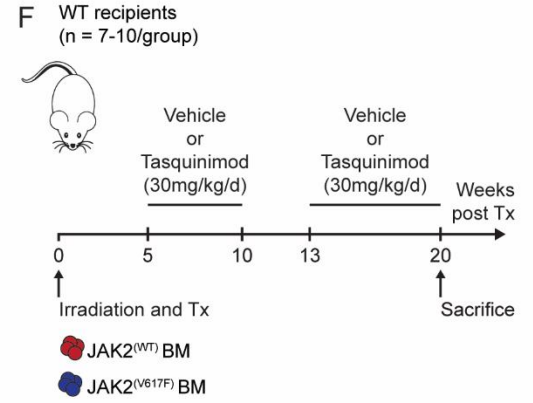
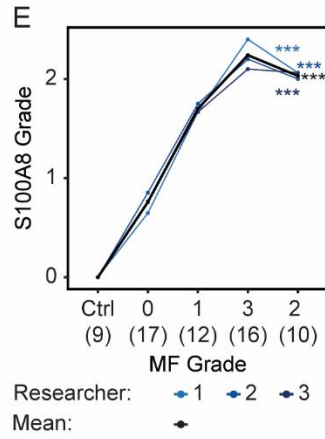
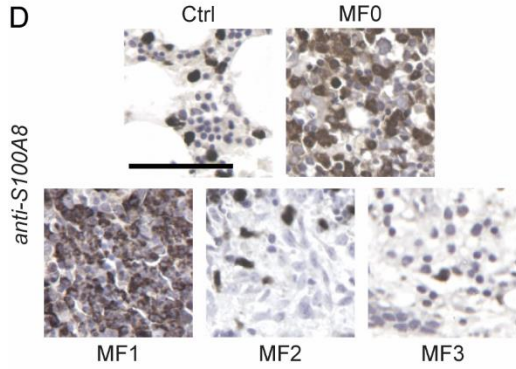


Figure S7: Validation of S100A8 as potential marker of disease progression and therapeutic target in the niche (related to Figure 7)

(A) Patient demographics and disease relevant data of the patient cohort used to measure S100A8 plasma levels. Data is shown as absolute number and relative frequency or as mean \pm SEM. Calculations were performed on all patients, where sufficient clinical data was available. **(B)** Pearson Correlation between the S100A8 Plasma levels as measured by ELISA and the leukocyte count in the peripheral blood. Analysis was performed on all patients, where the corresponding leukocyte count was documented. **(C)** Patient demographics and disease relevant data of the patients whose bone marrow slides were used for S100A8 immunohistochemistry. Data is shown as absolute number and relative frequency or as mean \pm SEM. Calculations were performed on all patients, where sufficient clinical data was available. **(D)** Representative images of S100A8 positivity in the hematopoietic compartment of patient bone marrow. Scale bar: 50 μ m. **(E)** Trend analysis of S100A8 gradings for different MF grades across independent assessments. Depicted is the median grade for each MF grade or control assessed by a single researcher. The mean across all 3 assessments is shown in black as reference. p-values were calculated for each researcher independently and corrected for multiple hypothesis testing by the Benjamini–Hochberg procedure. **(F)** Mice transplanted with JAK2^{V617F}- or JAK2^{WT}-transduced ckit⁺ cells received Tasquinimod (ABR-215050) treatment (30mg/kg/day in drinking water) or vehicle treatment from 5 weeks until 10 weeks, and from 13 until 20 weeks post-transplant. n = 7-10/group. **(G)** Hemoglobin levels and **(H)** Platelet counts of WT mice transplanted with either JAK2^{V617F} (blue) - or JAK2^{WT} overexpressing HSPCs (red) each either treated with Tasquinimod 30mg/kg/day or Vehicle control. A two-way repeated measures ANOVA was performed to evaluate differences between the groups at different timepoints. The effect of the treatment was analyzed at each timepoint. Pairwise comparisons were analyzed by estimated marginal means. **(I)** Representative images of bone marrow reticulin staining in mice transplanted with either JAK2^{V617F}- or JAK2^{WT}-transduced ckit⁺ cells receiving Tasquinimod or vehicle treatment. scale bar: 250 μ m. **(J)** Representative images of HE staining in the bone marrow of control and Tasquinimod-treated mice. scale bar: 100 μ m. **(K)** Mesenchymal stromal cells were isolated and cultured in the presence of either PBS, TGF-b +vehicle control (DMSO) or TGF-b + Tasquinimod for 72h. Cells were stained for α -smooth muscle actin (α -SMA). Representative confocal images for each condition are depicted. **(L)** Quantification of α -SMA⁺ cells per HPF as percentage of total number of cells. Experimental triplicates (n=3) were manually counted by 3 independent researchers. Data is presented as mean \pm SEM. Statistical significance was estimated by One-Way-ANOVA with *post-hoc* Tukey's HSD.

Table S6: Primer List (related to Supplemental Figure S2, S5)

Transcript	Forward	Reverse	Source
Acta2	CTGACAGAGGCACCACTGAA	CATCTCCAGAGTCCAGCACA	
Col1a1	ACGGCTGCACGAGTCAAC	GGCAGGCGGGAGGTCTT	
Cxcl12	CACTCCAAACTGTGCCCTTCA	CACTTTAATTTCCGGTCAATGC	
Gapdh	GGTGAGGCCGGTGCTGAGTATG	GACCCGTTTGCTCCACCCTTC	
S100b	AACAACGAGCTCTCTCACTTCC	CTCCATCACTTTGTCCACCA	Quintes S et al., 2016
p75ntr	CGGTGTGCGAGGACACTGAGC	TGGGTGCTGGGTGTTGTGACG	Quintes S et al., 2016